Development of the first non-hydroxamate selective HDAC6 degraders

Tim Keuler,‡[a] Beate König,‡[a] Nico Bückreiß,‡[a] Fabian B. Kraft,[a] Philipp König,[a] Christian Steinebach,[a] Gerd Bendas,*[a] Michael Gütschow*[a] and Finn K. Hansen*[a]

[a] *Pharmaceutical Institute, University of Bonn, An der Immenburg 4, 53121 Bonn, Germany.*

‡ These authors contributed equally.

Correspondence: gbendas@uni-bonn.de

guetschow@uni-bonn.de

finn.hansen@uni-bonn.de

Abstract

The targeted degradation of histone deacetylase 6 (HDAC6) by heterobifunctional degraders constitutes a promising approach to treat HDAC6-driven diseases. Previous HDAC6 selective degraders utilised a hydroxamic acid as a zinc-binding group (ZBG) which features mutagenic and genotoxic potential. Here we report the development of a new class of selective HDAC6 degraders based on a difluoromethyl-1,3,4-oxadiazole (DFMO) warhead as ZBG.

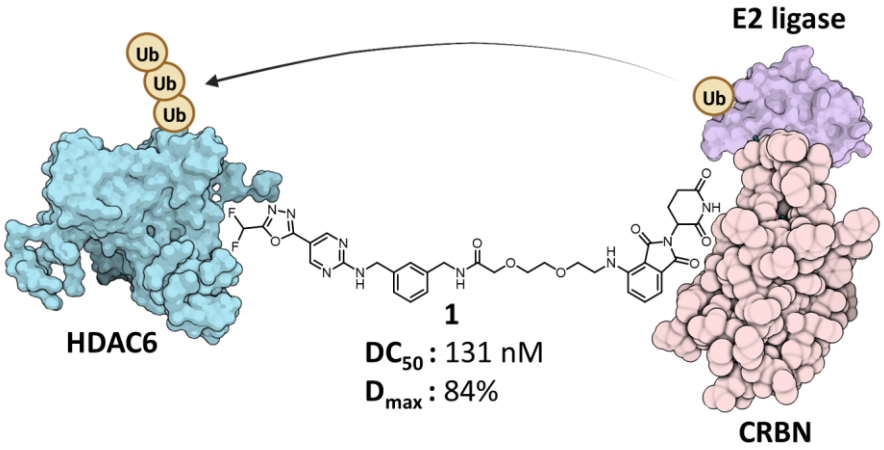

Main text

Histone deacetylases (HDACs) are considered important epigenetic drug targets for the therapy of haematological and solid cancers.[1] Four HDAC inhibitors (HDACi; vorinostat, romidepsin, belinostat, and panobinostat) have received regulatory approval by the FDA for treating T-cell lymphoma and multiple myeloma. However, all approved HDACi do not possess selectivity for a specific HDAC isoform.[1] Due to their lack of isoform-selectivity, such unselective HDACi often cause suffering from serious adverse effects.[1] Thus, to optimise the risk-benefit profile of HDACi, there is urgent need to develop isoform-specific HDAC inhibitors.

HDAC6 is overexpressed in various cancer types and modulates the activity of several non-histone proteins such as α-tubulin, cortactin, and Hsp90.[2] Since the knockout of HDAC6 in mice did not produce significant defects, HDAC6 inhibitors are considered to exhibit improved safety profiles compared to pan-HDACi.[3] HDAC6 is structurally unique and comprises two active catalytic domains (CD1 and CD2) as well as a zinc finger functioning as an ubiquitin-binding domain (UBD). Classical HDAC6-selective inhibitors impede CD2 but do not interfere with enzymatic and non-enzymatic functions facilitated by CD1 or the UBD.[1] Hence, the chemical knockdown of HDAC6 may be superior to the sole inhibition of CD2.

Hijacking the ubiquitin-proteasome system (UPS) with proteolysis-targeting chimeras (PROTACs) is an emerging new therapeutic modality, which enables the targeted degradation of a protein of interest (POI). These heterobifunctional molecules consist of an E3 ligase ligand and a recognition motif for the POI connected by a suitable linker, thereby acting as proximity inducers.[4,5] The formation of a POI : PROTAC : E3 ligase ternary complex initiates the polyubiquitination of the POI, leading to its proteasomal degradation.[2] In 2018, Schiedel *et al.*[6] and Yang *et al.*[7] reported the first Sirt2 and HDAC6 PROTACs, respectively. Several selective HDAC6 degraders have been disclosed in the past years, including compounds based on the HDAC6 inhibitor nexturastat A and the pan-HDACi crebinostat.[7-12] All selective HDAC6 PROTACs reported so far contain a hydroxamate zinc-binding group (ZBG) which coordinates the zinc ion in the active site

of HDAC6 CD2.[7-12] Although hydroxamic acids have been successfully utilised as ZBGs in approved HDACi as well as in numerous late-stage clinical candidates, they may transform *via* Lossen rearrangements into mutagenic and highly reactive electrophilic species such as isocyanates susceptible to react with naturally-occurring nucleophiles.[13] To avoid such mutagenic and genotoxic potential, new ZBGs are desirable for HDAC PROTAC development.[13] Herein, we report the first non-hydroxamate, selective HDAC6 PROTACs that contain difluoromethyl-1,3,4-oxadiazole warheads as ZBGs.

Selective HDAC6 inhibitors typically consist of a hydroxamate ZBG connected to a short benzyl or 4-aminophenyl linker and a bulky, rigid cap group that confers isoform selectivity. A few alternative ZBGs, for example, mercaptoacetamides, thiols, and trifluoromethyl ketones enabled potent HDAC6 inhibition but lower selectivity than hydroxamic acids.[14] In 2018, Yates[15] disclosed a new type of highly potent HDAC6 selective inhibitors based on pyrimidine linkers and the 2-(difluoromethyl)-1,3,4-oxadiazole (DFMO) group as ZBG (for representative structures, see Fig. S1, ESI). Inspired by this scaffold, we designed the *meta*- and *para*-connected HDAC6 ligands **I** and **II** (Fig. 1A) containing acetyl groups that mimic the PROTAC attachment points. Docking studies (Fig. S2, ESI) to investigate their potential as POI ligands showed the acetyl group of the *meta*-substituted derivative **I** solvent-exposed (Fig. 1B), indicating an appropriate exit vector to assemble PROTACs. In turn, the predicted binding mode for the *para*-substituted analogue **II** suggests that the acetyl group binds in the proximity of Thr563 and Met567 (Fig. S3, ESI). However, it seems sufficiently solvent-exposed. We thus decided to pursue both *meta*- and *para*-connected PROTACs and designed degraders that are capable of recruiting the well-studied E3 ubiquitin ligases cereblon (CRBN) and von Hippel-Lindau (VHL) (Fig. 1C).

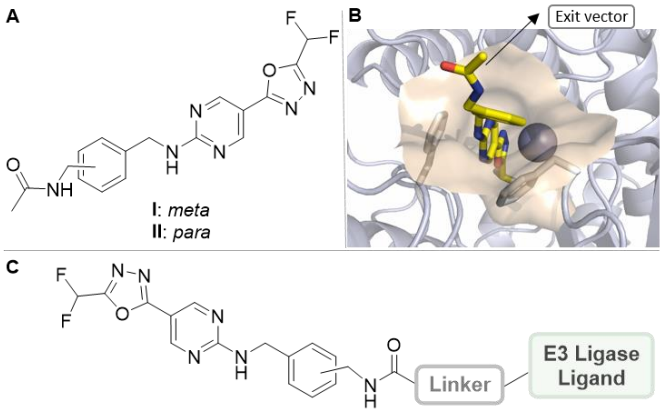

Fig. 1. (A) HDAC6 ligands **I** and **II** with possible PROTAC attachment points in *meta* and *para* position. **(B)** Docking pose of ligand **I** in the CD2 of HDAC6 (PDB: 5EDU).[16] The catalytic Zn^{2+}-ion is shown as gray sphere. **(C)** Designed *meta*- and *para*-connected PROTACs intended to degrade HDAC6.

For the synthesis of the required DFMO-based HDAC6 ligands (Scheme 1) the mono-Boc-protected bis(aminomethyl)benzenes **7** and **8** were converted to the orthogonally protected building blocks **9** and **10**. After Boc-deprotection, the nucleophilic aromatic substitution of 2-chloropyrimidine-5-carbonitrile afforded the carbonitrile intermediates **11** and **12**, which were subjected to the reaction with sodium azide to provide **13** and **14**. For the preparation of the desired HDAC6 ligands **15** and **16**, the tetrazoles **13** and **14** were reacted with difluoroacetic anhydride (DFAA) to generate the DFMO group *via* a Huisgen 1,3,4-oxadiazole synthesis.[17]

The cereblon-based PROTAC precursors were obtained *via* the synthetic route depicted in Scheme 2. First, a PEG-containing precursor (**26**) with pomalidomide as a cereblon binding unit was prepared. For this purpose, 2-(2-aminoethoxy)ethanol (**17**) was Cbz-protected to **18**, which was elongated through *O*-alkylation with *tert*-butyl bromoacetate. The resulting orthogonally protected linker **19** underwent catalytic hydrogenolysis to give the primary amine **20**. This was employed in a nucleophilic substitution reaction with 4- fluorothalidomide (**25**) to yield **26**.[18]

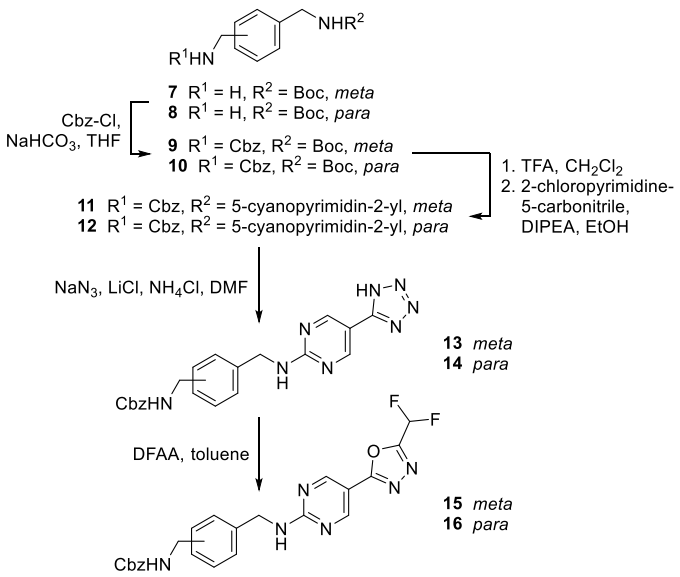

Scheme 1. Synthesis of HDAC6 ligands with a 2-(difluoromethyl)-1,3,4-oxadiazole-based zinc-binding group.

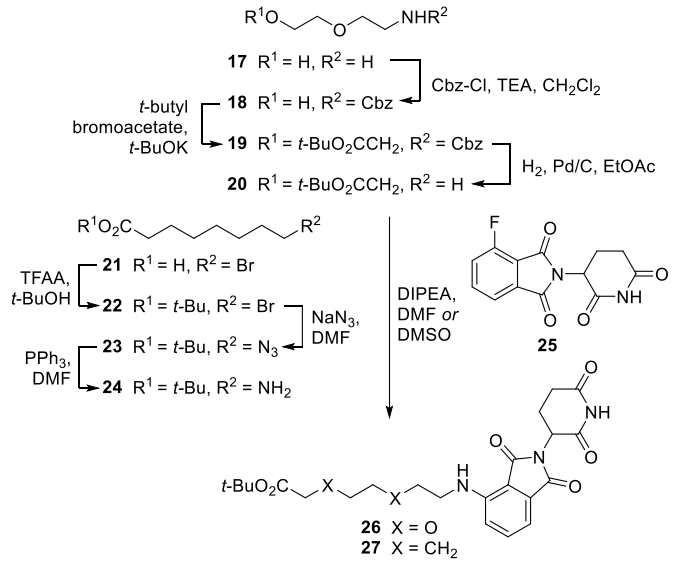

Scheme 2. Synthesis of precursors for cereblon-based PROTACs.

To evaluate the impact of compound polarity on degradation potency, we conceived the cereblon-based PROTAC precursor **27** with an alkylidene chain of equal length. Starting with 8-bromooctanoic acid (**21**), an esterification with *tert*-butanol and trifluoroacetic anhydride was performed,[19] leading to **22**, which was transformed into the azide **23**, followed by a

Staudinger reaction. The amine **24** was then conjugated with 4-fluorothalidomide (**25**) to obtain the second cereblon-based PROTAC precursor **27**.

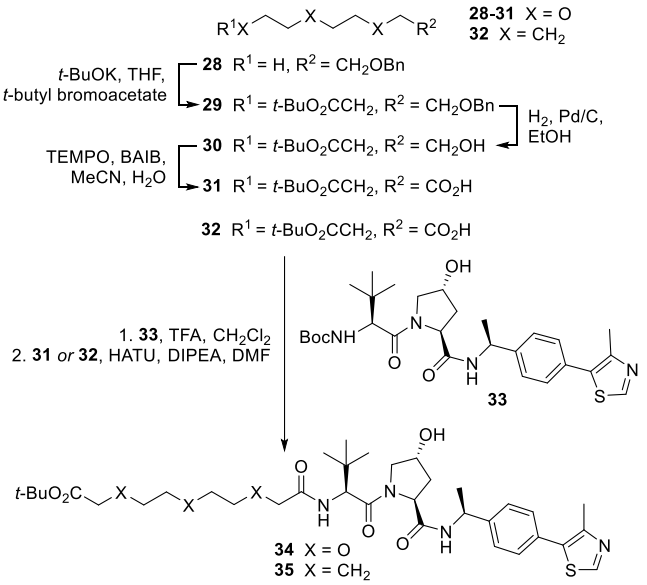

Scheme 3. Synthesis of precursors for VHL-based PROTACs.

The preparation of the VHL-based PROTAC precursor **34** (Scheme 3) started with the *O*-alkylation of benzyl ether **28** to give **29**, followed by hydrogenolytic deprotection. The resulting alcohol **30** was oxidised with (diacetoxyiodo)benzene (BAIB) and TEMPO to the carboxylic acid **31**. The Boc-protected VHL ligand **33** was synthesised in a convergent approach (Scheme S1, ESI).[20] Upon deprotection of **33**, it was linked to **31** in a uronium salt-mediated coupling to achieve the VHL-based PROTAC precursor **34**. The analogue alkylidene precursor **35** was similarly obtained from unilaterally esterified undecanedioic acid **32**.

After hydrogenolytic deprotection of the HDAC6 ligands **15** and **16** and TFA-promoted deprotection of the PROTAC precursors **26**, **27**, **34** and **35**, respectively, the HDAC6 degraders **1-6** were finally assembled through amide coupling (Table 1). An overview on important physicochemical properties (molecular weight, lipophilicity, plasma protein binding, number of rotatable bonds, polar surface area) to assess the drug-likeliness of the degraders is provided, too. Notably, introduction of oxygen atoms into the linker reduced both lipophilicity and plasma protein binding values.

PROTACs **1-6** were first assayed for their in vitro inhibitory activity against HDAC6 using ZMAL (Z-Lys(Ac)-AMC) as a fluorogenic substrate. The FDA-approved HDACi vorinostat was used as

a positive control. All PROTACs demonstrated HDAC6 inhibitory properties with IC_{50} values ranging from 0.590 to 1.86 µM (Table 1). The class I isoforms HDAC1-3 are the major source of cytotoxicity of HDAC inhibitors and degraders.[21] Consequently, to analyse the selectivity profile of **1-6**, all PROTACs were further screened for their inhibitory potency at HDAC1-3. Strikingly, PROTACs **1-6** were inactive against HDAC1-3 (IC_{50} > 30 µM, Table S1, ESI), thereby confirming their selectivity for HDAC6 over HDAC1-3.

Table 1. Final assembly of HDAC6-addressing PROTACs and overview on their biological activities and physicochemical properties.

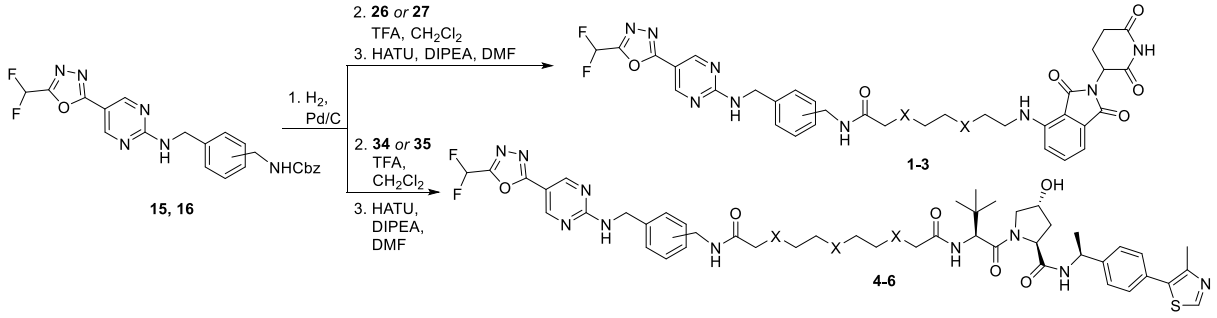

cmpd	aminomethyl position	X	HDAC6 IC_{50} (µM)	D_{max} (%) [a]	M_r (g/mol)	elog $D_{7.4}$ [b]	HAS (%) [c]	TPSA (Å²) [d]	NRotB [e]
1	*meta*	O	0.643 ± 0.204	84	734	2.5	88	220	18
2	*meta*	CH_2	0.590 ± 0.133	17	730	3.3	95	201	18
3	*para*	O	1.86 ± 0.250	70	734	2.4	91	220	18
4	*meta*	O	0.686 ± 0.113	74	963	2.6	90	273	28
5	*meta*	CH_2	1.68 ± 0.255	43	957	3.3	95	246	28
6	*para*	O	1.59 ± 0.123	55	963	2.6	90	273	28

[a] D_{max}, maximal degradation. [b] Experimental distribution coefficient at pH 7.4. [c] Experimentally determined percentage of compound bound to human serum albumin. [d] Topological polar surface area. [e] Number of rotatable bonds.

In order to investigate whether the PROTACs **1-6** are capable of degrading HDAC6, we treated the multiple myeloma cell line MM.1S with 1 µM of each degrader for 24 hours. HDAC6 degradation was subsequently determined by western blot analysis. As summarised in Table 1 and Fig. 2A, all compounds demonstrated a pronounced degradation of HDAC6. The most substantial degradation was achieved by compound **1** from the CRBN-recruiting series, whereas compound **4** displayed the highest reduction of HDAC6 levels among the VHL-

recruiting PROTACs. Consequently, compounds **1** and **4** were selected for the following in-depth biological evaluation.

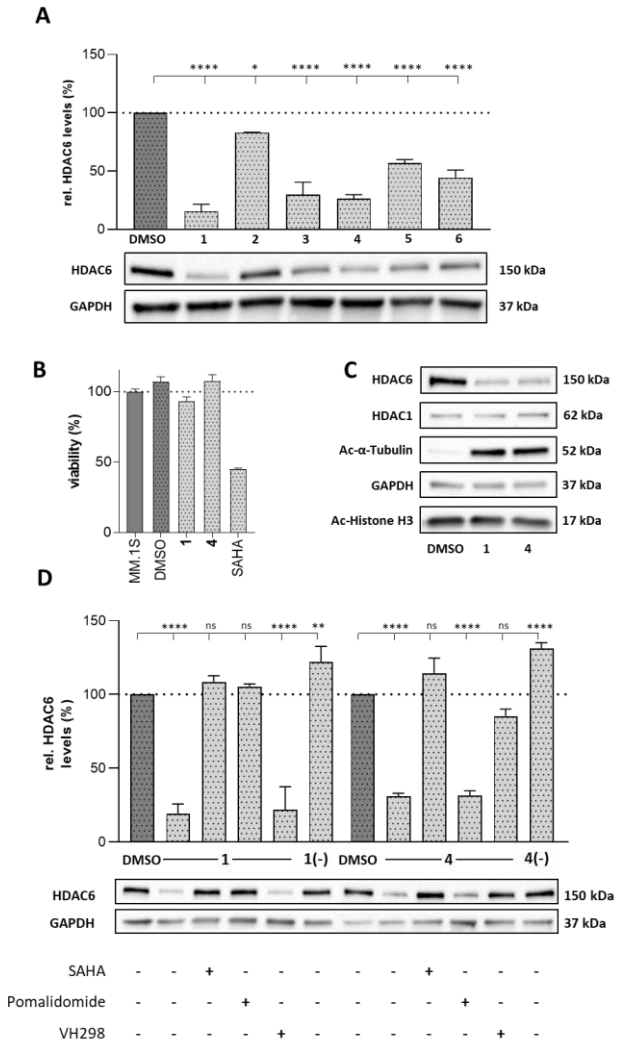

Fig. 2. Characterization of non-hydroxamate HDAC6 PROTACs. **(A)** Western blot analysis of whole cell lysates of MM.1S cells after treatment with compounds **1-6** at 1 µM for 24 h or with vehicle control (DMSO). **(B)** Investigation of potential cytotoxicity mediated by PROTACs **1** and **4** at a concentration of 1 µM and after an incubation time of 72 h in MM.1S cells. SAHA (1 µM) was used as cytotoxic control. **(C)** Protein levels of HDAC1, HDAC6, acetyl-α-tubulin, acetyl-histone H3 and GAPDH were quantified by western blot analysis after an incubation of 24 h with respective PROTACs **1** and **4** (1 µM) in comparison to vehicle control (DMSO). **(D)** MM.1S cells were pre-treated with pomalidomide (10 µM), VH298 (10 µM), SAHA (1 µM) or vehicle control (DMSO) for 30 min and then treated for 24 h with 1 µM of **1** and **4**, respectively. Statistical analysis was performed by using one-way ANOVA following Dunnett´s test. Statistical significance was indicated with asterisks (* = $p < 0.05$; ** = $p < 0.01$; *** = $p < 0.001$; **** = $p < 0.0001$).

In the first step, MM.1S cells were incubated for 24 hours with several PROTAC concentrations to determine the half-degrading concentrations ($DC_{50,24h}$) of both degraders (Fig. S4, ESI). Notably, **1** ($DC_{50,24h}$ = 131 nM) and **4** ($DC_{50,24h}$ = 171 nM) reduced HDAC6 levels with DC_{50} values in the nanomolar concentration range. To exclude possible cytotoxic effects of the PROTACs, cell viability of MM.1S cells was detected by CellTiter-Glo 2.0 luminescent cell viability assay, confirming that neither **1** nor **4** caused any considerable reduction in cell viability (Fig. 2B).

Additional experiments were conducted to investigate the selectivity profile of both PROTACs (Fig. 2C). To this end, HDAC1 was selected as a representative class I HDAC isoform. Although both compounds degraded HDAC6 remarkably, they had no impact on HDAC1 levels. To further confirm the HDAC6 selectivity, western blot analysis of acetylated histone H3 (a marker of reduced HDAC1-3 activity) and acetylated α-tubulin (a marker of reduced HDAC6 activity) were performed. In good agreement with the results of the fluorogenic enzyme assay (Table S1, ESI), the degraders **1** and **4** led to selective upregulation of acetyl-α-tubulin and caused no hyperacetylation of histone H3. Consequently, these results verify the potency and HDAC6 selectivity of both PROTACs.

To confirm that degradation of HDAC6 is mediated by ternary complex formation, MM.1S cells were pretreated with the CRBN-ligand pomalidomide or the VHL-ligand VH298, followed by the addition of the PROTACs. As expected, degradation of HDAC6 induced by **1** (CRBN-recruiting) was blocked by pomalidomide, while VH298 only prevented the degradation activity of **4** (VHL-recruiting). Similarly, pretreatment with vorinostat (SAHA) rescued HDAC6 from degradation (Fig. 2D). To provide further evidence that HDAC6 degradation relied on ternary complex formation, we synthesised the non-degrading controls **1(-)** and **4(-)** by methylation of the glutarimide or by inversion of the stereochemistry at the hydroxyproline to abolish the binding to the respective E3 ligase (see ESI for structures and synthetic details). As illustrated in Fig. 2D, both control compounds showed no reduction in HDAC6 levels.

In summary, we have designed, synthesised and evaluated the first non-hydroxamate HDAC6 degraders based on a difluoromethyl-1,3,4-oxadiazole warhead as ZBG. Western blot analysis demonstrated that the PROTACs **1** (CRBN-recruiting) and **4** (VHL-recruiting) are capable of degrading HDAC6 in a potent and selective manner. Competition experiments with vorinostat and pomalidomide or VH298 confirmed that the degradation of HDAC6 occurs via ternary complex formation and this was further supported by the inclusion of the non-degrading

controls **1(-)** and **4(-)**. Considering the involvement of HDAC6 in various pathological conditions, the selective HDAC6 degraders reported in this work may be useful pharmacological tools to dissect the function of HDAC6 in cancer and non-oncological diseases.

Supplementary Information

Electronic Supplementary Information (ESI) available: Supplementary Figures, Schemes and Tables, experimental procedures, ^{1}H NMR, ^{13}C NMR and MS data, docking protocols.

Acknowledgements

T.K. was supported by a fellowship from the Jürgen Manchot Foundation, Düsseldorf, Germany.

Conflicts of interest

There are no conflicts to declare.

References

1 R. Jenke, N. Reßing, F. K. Hansen, A. Aigner and T. Büch, *Cancers*, 2021, **13**, 634.

2 F. Fischer, L. A. Alves Avelar, L. Murray and T. Kurz, *Future Med*. *Chem.*, 2021, **14**, 143–166.

3 Y. Zhang, S. Kwon, T. Yamaguchi, F. Cubizolles, S. Rousseaux, M. Kneissel, C. Cao, N. Li, H.-L. Cheng, K. Chua, D. Lombard, A. Mizeracki, G. Matthias, F. W. Alt, S. Khochbin and P. Matthias, *Mol. Cell. Biol.*, 2008, **28**, 1688–1701.

4 R. Chopra, A. Sadok and I. Collins, *Drug Discov. Today Technol.*, 2019, **31**, 5–13.

5 I. Sosič, A. Bricelj and C. Steinebach, *Chem. Soc. Rev.*, 2022, **51**, 3487-3534.

6 M. Schiedel, D. Herp, S. Hammelmann, S. Swyter, A. Lehotzky, D. Robaa, J. Oláh, J. Ovádi, W. Sippl and M. Jung, *J. Med. Chem.*, 2018, **61**, 482–491.

7 K. Yang, Y. Song, H. Xie, H. Wu, Y. T. Wu, E. D. Leisten and W. Tang, *Bioorg. Med. Chem. Lett.*, 2018, **28**, 2493–2497.

8 H. Wu, K. Yang, Z. Zhang, E. D. Leisten, Z. Li, H. Xie, J. Liu, K. A. Smith, Z. Novakova, C. Barinka and W. Tang, *J. Med. Chem.*, 2019, **62**, 7042–7057.

9 H. Yang, W. Lv, M. He, H. Deng, H. Li, W. Wu and Y. Rao, *Chem. Commun.*, 2019, **55**, 14848–14851.

10 L. Sinatra, J. J. Bandolik, M. Roatsch, M. Sönnichsen, C. T. Schoeder, A. Hamacher, A. Schöler, A. Borkhardt, J. Meiler, S. Bhatia, M. U. Kassack and F. K. Hansen, *Angew. Chem. Int. Ed.*, 2020, **59**, 22494–22499.

11 K. Yang, H. Wu, Z. Zhang, E. D. Leisten, X. Nie, B. Liu, Z. Wen, J. Zhang, M. D. Cunningham and W. Tang, *ACS Med. Chem. Lett.*, 2020, **11**, 575–581.

12 Y. Xiong, K. A. Donovan, N. A. Eleuteri, N. Kirmani, H. Yue, A. Razov, N. M. Krupnick, R. P. Nowak and E. S. Fischer, *Cell Chem. Biol.*, 2021, **28**, 1514-1527.e4.

13 S. Shen and A. P. Kozikowski, *ChemMedChem*, 2016, **11**, 15–21.

14 A. Frühauf and F.-J. Meyer-Almes, *Molecules*, 2021, **26**, 5151.

15 C. M. Yates, US Pat., 2018/0256572 A1, 2018.

16 Y. Hai and D. W. Christianson, *Nat. Chem. Biol.*, 2016, **12**, 741–747.

17 R. Huisgen, J. Sauer and H. J. Sturm, *Angew. Chem. Int. Ed.*, 1958, **70**, 272–273.

18 C. Steinebach, H. Kehm, S. Lindner, L. P. Vu, S. Köpff, Á. L. Mármol, C. Weiler, K. G. Wagner, M. Reichenzeller, J. Krönke and M. Gütschow, *Chem. Commun.*, 2019, **55**, 1821–1824.

19 C. Jacquot, C. M. McGinley, E. Plata, T. R. Holman and W. A. van der Donk, *Org. Biomol. Chem.*, 2008, **6**, 4242–4252.

20 M. Wang, J. Lu, M. Wang, C. Yang and S. Wang, *J. Med. Chem.*, 2020, **63**, 7510–7528.

21 Y. Depetter, S. Geurs, R. De Vreese, S. Goethals, E. Vandoorn, A. Laevens, J. Steenbrugge, E. Meyer, P. de Tullio, M. Bracke, M. D'hooghe and O. De Wever, *Int. J. Cancer*, 2019, **145**, 735–747.